Aerosol and Air Quality Research, 13: 730–738, 2013

ISSN: 1680-8584 print / 2071-1409 online
doi: 10.4209/aaqr.2012.07.0177

Effects of Sulfur, Nitric Acid, and Thermal Treatments on the Properties and Mercury Adsorption of Activated Carbons from Bituminous Coals

Hsing-Cheng Hsi[1*], Mark J. Rood[2], Massoud Rostam-Abadi[2,3], Yu-Min Chang[1]

[1] *Institute of Environmental Engineering and Management, National Taipei University of Technology, No. 1, Sec. 3, Chung-Hsiao E. Rd., Taipei 106, Taiwan*
[2] *Department of Civil and Environmental Engineering, University of Illinois, 205 N. Mathews Ave., Urbana, IL 61801, USA*
[3] *Illinois State Geological Survey, 615 E. Peabody Dr., Champaign, IL 61820, USA*

ABSTRACT

The influences of sulfur, HNO_3, and thermal treatments on the properties and Hg adsorption of activated carbon (AC) derived from bituminous coals were evaluated. These ACs were impregnated with either polysulfide or elemental sulfur at 120, 200, and 600°C. Additional ACs were treated with HNO_3 at 95°C to incorporate oxygen functionalities, and then subjected to temperature-programmed desorption to 950°C to remove surface oxygen groups and create nascent active sites on the AC surface. Polysulfide and elemental sulfur impregnation at < 200°C did not improve Hg^0 adsorption. However, improvement in $HgCl_2$ adsorption by up to 97% was observed. Elemental sulfur impregnation at 600°C enhanced Hg^0 and $HgCl_2$ adsorption by up to 42% and 404%, respectively, for ACs derived from a low-organic-sulfur coal. Improvements in Hg^0 adsorption for ACs from high-organic-sulfur coals were not observed after sulfur impregnation. HNO_3 and thermal treatments reduced Hg-active groups such as sulfur. Oxygen surface groups and the nascent carbon sites appeared to be more reactive towards other flue gas components than Hg, because HNO_3 and thermal treatments led to a reduction in Hg^0 and $HgCl_2$ adsorption. These results suggest that AC's physical and chemical properties after sulfur treatment influence Hg^0 adsorption, while $HgCl_2$ adsorption is mainly affected by AC's chemical characteristics.

Keywords: Adsorbent; Mercury; Sulfur; HNO_3; Thermal treatment.

INTRODUCTION

Hg consisting of Hg^0, Hg^{2+}, and organic Hg is a toxic pollutant that bioaccumulates in human and wildlife through the food chain (Bittrich *et al.*, 2011a, b). The United States' Clean Air Act Amendments of 1990 list Hg as one of the original 188 hazardous air pollutants (HAPs). Hg can travel globally upon release to the environment from both natural and anthropogenic sources. Coal-fired power plants (CFPPs) have been identified as the largest single anthropogenic source category in most countries (Pacyna *et al.*, 2010; Fang *et al.*, 2012; Wu *et al.*, 2012). Low-concentration Hg (1–10 ppb_v) in CFPP flue gas is difficult to separate from the flue gas stream. Numerous approaches have been developed to remove low-concentration Hg from coal combustion flue gases. These approaches are expected to respond to the new Mercury and Air Toxics Standards (MATS) that were announced by USEPA in March 2011 and finalized in December 11, 2011 for coal-and oil-fired electric generating units (U.S. Environmental Protection Agency website, 2011).

Adsorption by porous carbonaceous materials is a promising technique to remove low-concentration Hg from CFPP gas streams. Efforts have been made to increase removal efficiency of activated carbon (AC) for both Hg^0 and Hg^{2+} via a carbon fixed bed or a powder injection approach (Staudt and Jozewicz, 2003). Sulfur impregnation has been shown to increase the Hg^0 adsorption capacity of ACs (Krishnan *et al*., 1994; Korpiel and Vidic, 1997; Liu *et al*., 1998, 2000; Hsi *et al*., 2001, 2002; Vitolo and Seggiani, 2002; Feng *et al.*, 2006a, b; Ho *et al.*, 2008). Adsorption onto sulfur-impregnated ACs at low temperature (i.e., < 150°C) was suggested to be the most mature technology for direct capture of gaseous Hg in coal gasification processes (Peise *et al*., 2008).

Previous research demonstrated that carbonaceous adsorbents with large Hg^0 adsorption capacities (> 5,000 μg-Hg per g-adsorbent; μg/g) can be prepared from select organic precursors by carbonizing, activating, and impregnating them with elemental sulfur between 200 and 650°C (Hsi *et al*., 2001, 2002, 2011). Impregnation at 400°C appeared

* Corresponding author. Tel.: +886 2 27712171 ext. 4126; Fax: +886 2 87732954
E-mail address: hchsi@ntut.edu.tw

optimal since the AC's porosity was preserved while active sulfur sites were added. Increasing bulk sulfur content did not necessarily ensure enhanced Hg^0 uptake. Feng *et al*. (2006b) agreed and reported that excess sulfur may block or fill the adsorbent's pores, hindering Hg^0 adsorption. They proposed that a sulfur monolayer maximizes Hg^0 adsorption capacity in microporous ACs.

Surface oxygen groups on AC can also be effective for enhancing Hg^0 adsorption. These groups are generally in the form of carboxylic, lactonic, phenolic, or quinonic on the AC surface (Bansal *et al.*, 1988). Matsumura (1974) demonstrated that Hg^0 adsorption capacities at 30°C increased approximately 20 times after oxidizing ACs with nitric acid. Li *et al*. (2003) also proposed that AC's Hg^0 adsorption capacity was correlated with lactone and carbonyl surface.

Removal of Hg^{2+} (e.g., $HgCl_2$, HgO) is also of interest because 50 to 80% of total vapor-phase Hg in flue gases generated from burning bituminous coals or high chlorine coals is in an ionic form (Carpi, 1997). Lancia *et al*. (1993) and Ghorishi and Sedman (1998) showed that temperature, $HgCl_2$ concentration, and relative gas-solid velocity strongly influenced the adsorption of $HgCl_2$ in fixed beds of $Ca(OH)_2$. They concluded that physisorption was the dominant mechanism for adsorption of $HgCl_2$. Karatza *et al*. (1998) also proposed that physisorption was the main mechanism for adsorption of $HgCl_2$ onto fly ash at < 150°C. However, at > 150°C, the $HgCl_2$ adsorption mechanism may fall into a "transition zone" between physisorption and chemisorption, based on a study using a mixture of AC and $Ca(OH)_2$ (Sorbalit; Märker-Gruppe, Germany).

In our previous study, ACs were prepared from high-sulfur coals and had comparable Hg^0 and $HgCl_2$ adsorption performance to that of a commercial AC (Hsi *et al*., 1998). This study further discusses the impacts of sulfur impregnation (elemental sulfur or polysulfide), HNO_3 treatment, followed by thermal treatments on the physical/chemical properties and Hg^0 and $HgCl_2$ adsorption by ACs derived from high- and low-organic-sulfur bituminous coals. Results from this work provide insight into the effectiveness of inherent and impregnated sulfur on Hg adsorption and an understanding of the role of AC surface oxygen groups and nascent carbon sites on Hg^0 and $HgCl_2$ adsorption in a simulated coal combustion flue gas.

MATERIALS AND METHODS

Preparation of Raw ACs

Two high-organic-sulfur (IBC107 and C2) and one low-organic-sulfur (IBC109) Illinois bituminous coals were used to prepare the AC samples (Table 1). IBC107 and IBC109 coals were obtained from the Illinois Basin Coal Sample Program and C2 was obtained from an active coal mine in Illinois. As-received coal samples were ground and sieved to between 0.21 and 1.00 mm in diameter. Bench-scale production of ACs was performed in a custom 5-cm ID fluidized-bed reactor with oxidation (air, 225°C), carbonization (N_2, 400°C), and then steam activation (50% H_2O/50% N_2, 825°C) (Hsi *et al*., 1998). Properties of the ACs are presented in Table 2.

Table 1. Ultimate and sulfur analyses of coal samples.

Property	Coal Sample		
	IBC107	C2 (wt%)	IBC109
Moisture	9.3	13.7	9.2
Ash[a, b]	11.5	9.7	8.3
Carbon[a]	68.2	72.0	75.2
Hydrogen[a]	4.9	5.2	5.0
Nitrogen[a]	1.2	1.3	1.7
Oxygen[a]	10.5	7.7	8.6
Sulfur[a]	3.7	4.1	1.2
Sulfatic Sulfur[a]	0.2	0.0	0.0
Pyritic Sulfur[a]	0.4	1.1	0.4
Organic Sulfur[a]	2.9	3.0	0.7
Total	100.0	100.0	100.0

[a] moisture free values.
[b] at 750°C with air.

Preparation of Sulfur-Impregnated ACs

Low-organic-sulfur IBC109 coal was used to prepare samples AC109-1 and AC109-2. AC109-2 was mechanically blended with 2 or 5 wt% powdered elemental sulfur, and heated at 200°C and ambient pressure for 6 h in a 5-cm (ID) tube furnace (Lindberg Model 59344) in ultra-high purity (UHP) N_2 (99.999%). The resulting ACs were designated as samples AC109-2-200S-2 and AC109-2-200S-5 (Table 2).

Sample AC109-2 was treated with polysulfide solution at 120°C and ambient pressure for 6 h. The polysulfide solution was prepared by mixing reagent-grade $Na_2S{\cdot}9H_2O$ with powdered elemental sulfur with a 2.5:1 mass ratio in deionized water and then heating the solution to 120°C until all the sulfur dissolved. The prepared ACs were subsequently washed with deionized water to remove residual polysulfide solution and dried in air at 105°C. The sulfur content of resulting samples were set to be 2 or 5 wt%, controlled by the concentration of polysulfide in solution used for impregnation. The resulting ACs were designated as AC109-2-120S-2 and AC109-2-120S-5 (Table 2).

Samples AC107, AC109-1, and AC109-2 were mechanically mixed with 20 wt% elemental sulfur and heated in the tube furnace at 600°C and ambient pressure for 3 h in UHP N_2. The resulting ACs were designated as AC107-600S, AC109-1-600S, and AC109-2-600S (Table 2).

Preparation of ACs with HNO_3 and Thermal Treatments

AC was subjected to a HNO_3 treatment to introduce oxygen groups onto the surface. Sample AC-C2 of 10 g was mixed with 100 mL of 45 vol% (v/v) reagent-grade $HNO_{3(aq)}$ and heated to 95°C at atmospheric pressure for 2.5 h. The resulting sample (designated as AC-C2-HNO_3) was rinsed with deionized water and dried at 105°C in air.

Samples AC-C2 and AC-C2-HNO_3 were subjected to temperature-programmed desorption (TPD) at a linear heating rate of 5 °C/min to 950°C in UHP N_2. TPD is used not only to quantify oxygen functional groups but also to generate nascent sites on the AC's surface. Thermal treatment at 950°C in oxygen-lean conditions develops nascent carbon sites due to desorption of surface oxygen functional groups.

Table 2. Chemical/physical characteristics and equilibrium Hg adsorption capacity of original, sulfur-, HNO_3-, and thermal-treated activated carbons.

Sample Code	Precursor Coal/CDAC	Sulfur Content (wt%)	Total Surface Area (m^2/g)	Micropore Surface Area (m^2/g)	Total Pore Volume (cm^3/g)	Micropore Volume (cm^3/g)	Hg^0 Adsorption Capacity (μg/g)	$HgCl_2$ Adsorption Capacity (μg/g)
AC107	IBC107	1.64	792	594	0.527	0.287	1925	463
AC109-1	IBC109	0.85	597	483	0.610	0.127	1126	97
AC109-2	IBC109	0.81	495	383	0.487	0.139	840	167
AC109-2-200S-5	AC109-2	5.72	29	0	0.037	0.000	699	293
AC109-2-120S-5	AC109-2	4.28	214	181	0.130	0.084	63	305
AC109-2-200S-2	AC109-2	2.36	337	296	0.190	0.137	519	297
AC109-2-120S-2	AC109-2	1.97	361	324	0.206	0.150	20	328
AC107-600S	AC107	12.7	645	464	0.415	0.298	1643	692
AC109-1-600S	AC109-1	12.4	510	413	0.301	0.187	1602	489
AC109-2-600S	AC109-2	12.0	360	291	0.197	0.133	963	682
AC-C2	C2	1.26	702	548	0.355	0.247	1758	657
AC-C2-HNO_3	AC-C2	0.84	590	441	0.324	0.205	334	64
AC-C2-HNO_3-TPD	AC-C2-HNO_3	0.96	671	493	0.398	0.230	355	264

The surface oxygen groups are generally formed on edge active sites that are much more reactive than the carbon atoms in the interior of the basal planes. Therefore, surface oxygen groups are predominantly located on the edges and their removal leaves carbon nascent sites containing unpaired electrons or residual valences, and therefore are more reactive than the basal planes for adsorbing organic and inorganic components, including hydrocarbons and SO_2 (Hoffman *et al.*, 1984; Daley *et al.*, 1997; Lizzio and DeBarr, 1997). ACs treated with HNO_3 were heated in a 2.5-cm ID stainless steel fixed-bed reactor with 0.5 standard L/min UHP N_2. The TPD process removes oxygen functional groups from the AC's surface as CO and CO_2 (Lizzio and DeBarr, 1997). CO_2 is released by decomposition of carboxylic or lactone groups at temperatures below 700°C. CO is released from decomposition of phenols, ethers, carbonyls and quinones at temperatures between 700 and 1000°C. The effluent TPD gas was analyzed for CO and CO_2 concentrations with an infrared analyzer (Rosemount Model 880). The total amount of surface oxygen (as wt% O_2) was determined from the amounts of CO and CO_2 evolved during a TPD experiment based on the concentration and gas flow rate. The resulting AC (designated as sample AC-C2-HNO_3-TPD) was collected for characterization and Hg adsorption tests.

During the HNO_3 and TPD treatments, some of the sulfur in AC was removed. The percent sulfur removal was calculated by:

$$S_{removal}\% = 100 - 100 \times (\frac{S_f}{S_0}) \times (Y) \quad (1)$$

where S_0 is the sulfur mass fraction of the original sample, S_f is the sulfur mass fraction of the product, and Y is the production yield, which is the product mass divided by the precursor mass.

Sample Characterization

Total surface area (S_{BET}), total pore volume (V_t), micropore (pore width < 2 nm) surface area (S_{micro}), micropore volume (V_{micro}), and pore size distribution of all ACs were determined by N_2 adsorption at 77 K (Micromeritics ASAP2400 analyzer). Samples were degassed at 0.013–0.026 atm vacuum and 150°C for 24 h before the N_2 adsorption measurements occurred between 0.001 and 1 atm. S_{BET} was calculated by the Brunauer-Emmett-Teller equation based on ASTM method D4820-96a. S_{micro} and V_{micro} were calculated from t-plot analyses using the Jura-Harkins equation: $t = [13.99/(0.0340 - \log(p/p_0)]^{0.5}$ (Lippens and de Boer, 1965). The range of relative pressures used to determine S_{micro} and V_{micro} was based on thickness t values between 0.45 and 0.8 nm. Micropore size distribution was determined using the 3-D model (Sun *et al*., 1998). Ultimate and sulfur analyses for all samples were measured by LECO MAC-d SC-32 systems according to ASTM methods D5373-93 and D4239-94, respectively. Least-squares analysis of sulfur K-edge X-ray absorption near-edge structure (S-XANES) spectra was used to quantify sulfur groups in select ACs. A detailed description of the principles and application of S-XANES spectroscopy is available elsewhere (Huggins *et al*., 1993).

Hg Adsorption Test

Bench-scale Hg^0 and $HgCl_2$ adsorption tests were performed at URS Corporation (Austin, TX) (Carey *et al*., 1998) and National Taipei University of Technology, Taiwan (Hsi *et al*., 2011). Briefly, Hg adsorption tests were performed at 150°C in a fixed-bed column (1.3 cm ID) that contained 20 –50 mg adsorbent in 10 g quartz sand (Fig. 1). The simulated CFPP gas stream fed to the fixed bed reactor was controlled at 1–1.2 standard (25°C and 1 atm) L/min with 1600 ppm_v SO_2, 50 ppm_v HCl, 12% CO_2, 7% H_2O, 6% O_2 and 50 ± 10 Hg^0 or $HgCl_2$ μg Nm^{-3}. Hg^0 and $HgCl_2$ were generated with certified Hg^0 and $HgCl_2$ permeation tubes (VICI Metronics) in a gas generator at 70 ± 0.1°C to ensure constant Hg diffusion rates. The effluent gas from the fixed-bed column flowed through heated lines to an impinger containing $SnCl_2$ that reduced any oxidizing Hg compounds to Hg^0.

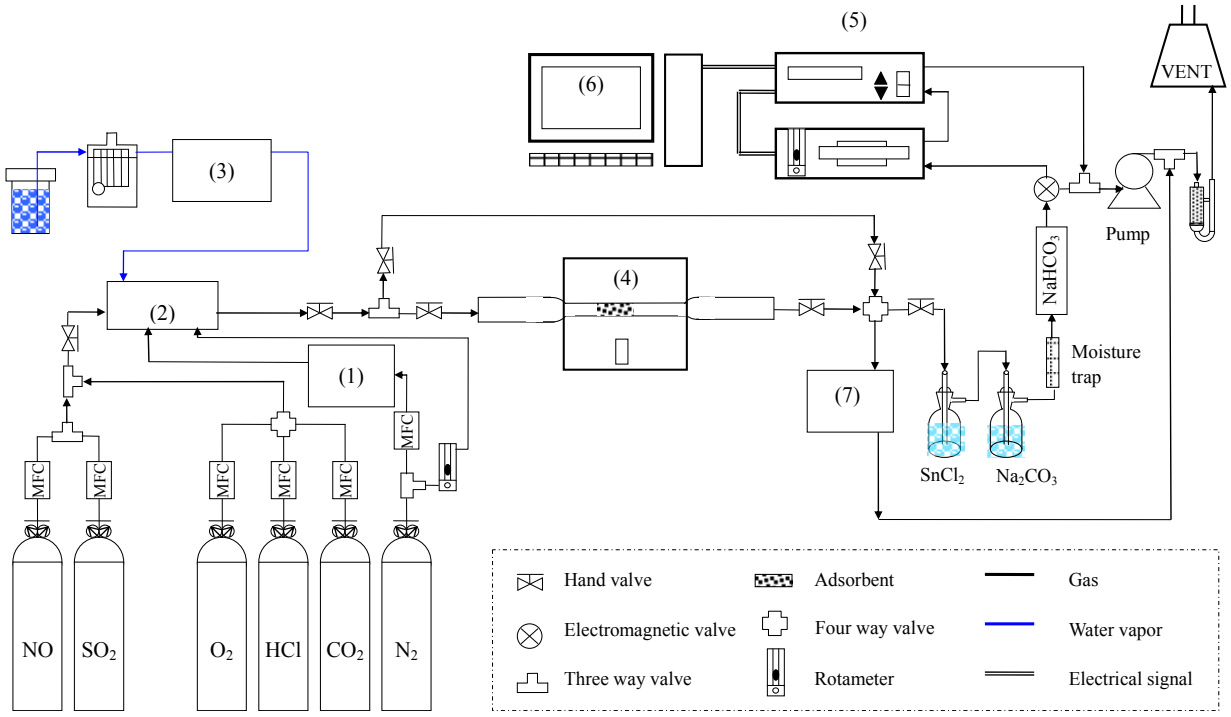

Fig. 1. Schematic diagram of Hg adsorption test devices: (1) Hg vapor generator; (2) gas mixing chamber; (3) moisture generator; (4) temperature-controlled adsorbent fixed bed; (5) gold amalgamation/CVAFS; (6) data acquisition system; (7) flue gas component analyzer.

The gas then flowed through an aqueous buffer solution (Na_2CO_3) to remove SO_2 and HCl and through a moisture trap (i.e., a nefion tube) to remove H_2O, thus protecting the downstream detector system. Gas exiting the impinger solutions flowed through a gold amalgamation column, where the Hg^0 in the gas was adsorbed and concentrated (< 100°C). After a fixed period of time, Hg^0 was thermally desorbed from the gold (> 750°C) and sent as a concentrated Hg^0 stream to a cold-vapor atomic absorption or a cold-vapor atomic fluorescence spectrophotometer for analysis.

Cumulative Hg adsorption (μg/g) at breakthrough was determined by:

$$\frac{m_i}{m_{adsorbent}} = \sum_{t=0}^{t'} \frac{(C_{i,in} - C_{i,out}) \times Q_g}{m_{adsorbent}} \Delta t \qquad (2)$$

where m_i is the mass of adsorbed Hg, $m_{adsorbent}$ is the total mass of adsorbent, t' is the adsorption time to achieve 100% breakthrough (i.e., equilibrium), $C_{i,in}$ is the inlet Hg concentration, $C_{i,out}$ is the outlet Hg concentration at time t, Q_g is the gas flow rate, and Δt is the time interval between measurements during the breakthrough test. Adsorption results for $HgCl_2$ were normalized to exclude the weight of adsorbed chlorine by multiplying the $HgCl_2$ adsorption capacities by 0.739, which is the molecular weight of Hg^0 divided by that of $HgCl_2$.

RESULTS AND DISCUSSION

Sulfur Impregnation at 120 and 200°C

Table 2 presents the chemical and physical characteristics of the original, sulfur-, HNO_3-, and thermal-treated ACs. Sample AC109-2 contained 0.81 wt% sulfur and its total sulfur content increased by 160 to 640% after polysulfide or elemental sulfur impregnation at 120 or 200°C. The sulfur contents of sample AC-109-2-200 prepared at 200°C were close to the total amount of sulfur introduced and inherent sulfur content of sample AC109-2, indicating that most of the added sulfur remained in the AC product. Polysulfide impregnation at 120°C was less effective, causing a smaller than expected increase in the bulk sulfur content.

The influence of sulfur impregnation on the physical properties of an AC depends on the amount of sulfur deposited onto the AC (Table 2). For the 2 wt% elemental-sulfur-impregnated (i.e., AC109-2-200S-2) and polysulfide-impregnated ACs (i.e., AC109-2-120S-2), S_{BET} and V_t were marginally affected (< 5% decrease compared to AC109-2). However, there were 92 and 40% decreases in S_{BET} for 5 wt% sulfur-impregnated ACs (AC109-2-200S-5 and AC109-2-120S-5, respectively). The 5 wt% polysulfide impregnation also affected the V_{micro} and micropore-size distributions of the resulting AC (Table 2). For example, the differential pore volume of the 5.5 Å peak for AC109-2 (0.097 $cm^3/g/Å$) decreased to 0.014 $cm^3/g/Å$ (AC109-2-120S-5), as the peak shifted to approximately 7 Å (Fig. 2), indicating that the impregnated sulfur molecules blocked and/or filled the 5.5 Å pore width.

ACs derived from high-organic-sulfur coal had larger Hg^0 and $HgCl_2$ adsorption capacities than those from the low-organic-sulfur coal (Table 2), in agreement with our earlier work (Hsi *et al*., 1998). Note that sample AC109-2

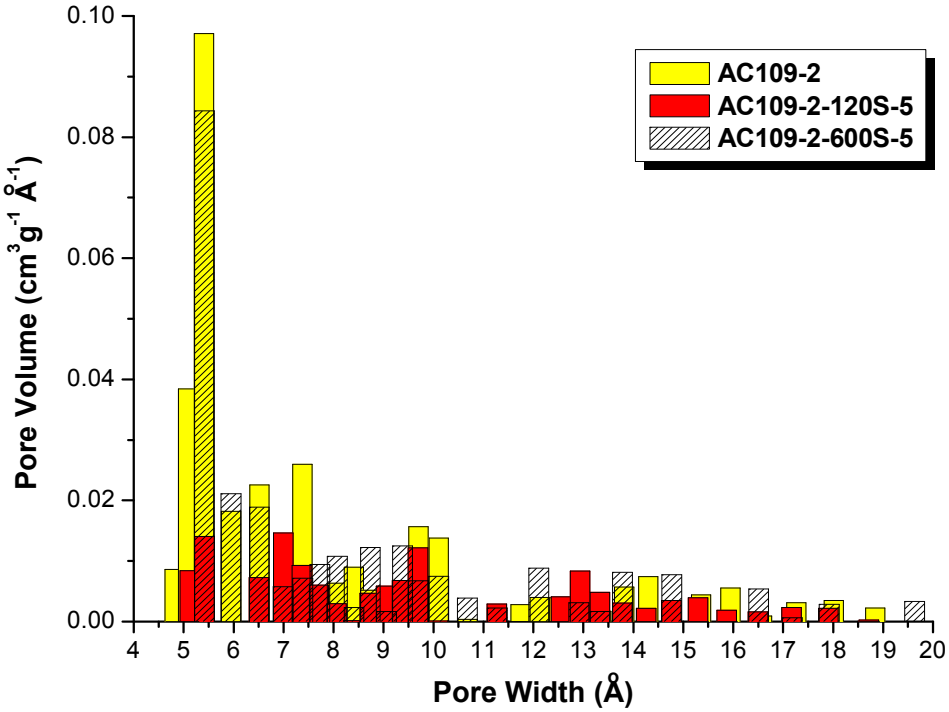

Fig. 2. Micropore-size distributions of original and sulfur-impregnated carbons.

showed a marked decrease in equilibrium Hg^0 adsorption capacity after sulfur impregnation at 120 or 200°C. AC109-2 had an equilibrium Hg^0 adsorption capacity of 840 μg/g, while the equilibrium capacity of the sulfur-treated samples was between 63 and 699 μg/g, reflecting a 17–93% decrease in adsorption capacity. Polysulfide impregnation caused an even larger reduction in Hg^0 adsorption capacity than elemental sulfur impregnation. The decrease in Hg^0 adsorption of treated ACs is explained by observing the forms of added sulfur and the changes in the AC's physical properties (Table 2). When elemental sulfur is impregnated into ACs at low temperatures (≤ 200°C), 99.96 mol% of the sulfur molecules exist as S_8 (77 mol%) or S_6 (23 mol%) rings (Tuller, 1954; Berkovitz, 1965). These sulfur forms are less reactive due to a lack of terminal sulfur atoms (Liu *et al.*, 1998). In addition, S_6 and S_8 rings with widths between 7.6 and 8.4 Å depending on if the molecule exists as a ring or chain may be too large to penetrate into AC's microporous structure, especially the ultra-micropores (pore width < 7 Å) (Hsi *et al.*, 2002). Consequently, these molecules may completely fill or block micropores (Table 2). Results also suggested that polysulfide molecules appeared to be less reactive than S_6 and S_8 for Hg^0 adsorption. These results indicate that the pronounced reduction in the Hg^0 adsorption capacity after low-temperature sulfur impregnation may stem from the changes in both physical and chemical properties of AC after low-temperature sulfur impregnation.

On the contrary, 120 and 200°C sulfur impregnation (except for AC109-2-120S-2) improved the equilibrium $HgCl_2$ capacities by up to 97% (Table 2). These results suggest that $HgCl_2$ adsorption is more affected by the chemical properties of AC (i.e., surface or bulk sulfur content) than the physical properties of AC (i.e., porosity).

Sulfur Impregnation at 600°C

We showed that sulfur impregnation at temperature ≥ 400°C enhanced Hg^0 adsorption of ACs (Hsi *et al.*, 2001, 2002, 2011). In this study, we chose 600°C as the impregnation temperature to deposit more organic sulfur functionalities on the AC surface (Hsi *et al.*, 2001). By doing so, the Hg adsorption results can be compared to those from ACs derived from high-organic-sulfur coals. Sulfur impregnation at 600°C increased the sulfur content of ACs from 0.81–1.64 wt% (AC107, AC109-1, and AC109-2) to 12–13 wt% (AC107-600S, AC109-1-600S, and AC109-2-600S) (Table 2). Notably, these samples showed a smaller decrease in S_{BET}, V_t and a smaller change in micropore size distribution compared to those of samples treated at 120 and 200°C. Clearly, sulfur impregnation at 600°C has less influence on the physical properties of ACs than the low temperature sulfur treatments used in this work.

Unlike the materials prepared at 120 and 200°C, low-organic-sulfur ACs (i.e., AC109-1 and AC109-2) impregnated with sulfur at 600°C showed considerable improvements in both Hg^0 and $HgCl_2$ adsorption capacities by up to 42% and 404%, respectively (Table 2). The same impregnation process used on the high-organic-sulfur AC (AC107) resulted in no improvement in equilibrium Hg^0 adsorption capacities, reducing from 1925 to 1643 μg/g, suggesting that ACs from high-organic-sulfur coals do not benefit from additional sulfur impregnation at these conditions (Hsi *et al.*, 1998). However, when the total sulfur content of AC107 increased from 1.64 to 12.7 wt% after sulfur impregnation, the equilibrium $HgCl_2$ adsorption capacities increased by 50%, from 463 to 692 μg/g. These findings again demonstrate the difference in adsorption mechanisms for Hg^0 and $HgCl_2$ with sulfur-impregnated ACs.

The form and reactivity of sulfur at high temperature (e.g., 600°C) is different than those at low temperatures (e.g., 120 and 200°C), causing differences in the properties and Hg adsorption capacities of the tested ACs. At 600°C, a large portion of sulfur molecules are in the form of S_2–S_4 (Berkovitz, 1965), which was estimated to have a diameter between 5.2 and 6.9 Å based on their molar volumes and assuming spherical sulfur molecules (Hsi *et al*., 2002). Unlike the aforementioned S_6 and S_8 rings that are suspected to mainly physisorb onto the AC surface at < 200°C, the smaller-sized S_2–S_4 molecules that possess active, terminal sulfur atoms can enter micropores, react with the carbon matrix, and form sulfur-carbon complexes. AC's existing atoms (e.g., sulfur, oxygen, hydrogen), functional groups, and unsaturated sites impact the effectiveness of sulfur impregnation (Puri and Hazra, 1971). At 600°C, impregnated sulfur can substitute onto existing functionalities, bond to unsaturated carbon atoms, or occupy activated sites due to carbon degradation during extended thermal treatment, as was shown using H_2S, CS_2, or SO_2 gases (Puri and Hazra, 1971; Blayden and Patrick, 1967). These reactions form organic sulfur on the AC surface. ACs impregnated with elemental sulfur at 600°C may undergo similar sulfur impregnation mechanisms as those using H_2S, CS_2 or SO_2 gases. S-XANES results showed that the content of organic thiophene, sulfone, and sulfoxide groups increased after 600°C sulfur impregnation (Table 3), supporting that carbon-sulfur bonds formed during the high temperature impregnation. S-XANES results also confirm that organic sulfur plays a critical role in Hg^0 adsorption since AC107 has negligible elemental sulfur content but high equilibrium Hg^0 adsorption.

The above results indicate that sulfur impregnation at 600°C can help increase Hg^0 adsorption capacity of a low-organic-sulfur ACs because it provides active organic sulfur sites without sacrificing the porous structure of the AC. Such approach is able to take advantage of the micropores to concentrate the Hg in the pores and organic sulfur functional groups to then react with the Hg. For $HgCl_2$ adsorption, it appears that sulfur groups, rather than micropores have a greater impact on $HgCl_2$ adsorption capacity.

Effects of HNO_3 Treatment

HNO_3 treatment is known to increase surface oxygen groups on ACs. Additionally, HNO_3 treatment is also an ASTM standard method (1988) to remove pyrite and sulfate from sulfur-containing materials, including coals. HNO_3 treatment oxidizes organic sulfide and thiophene into sulfoxide and sulfone in lignite coals (Maes *et al.*, 1996). The dissolution and transformation of sulfur functional groups after HNO_3 treatment may influence the $Hg^0/HgCl_2$ adsorption reactivity and capacity of ACs. In this study, the oxygen content of AC was estimated based on TPD results (Fig. 3). HNO_3 treatments increased the oxygen content of AC-C2 from 1.9 to 16.9 wt% as O_2. The surface oxygen groups evolved from the AC as CO_2 with a peak at 270°C and shoulders between 100 and 800°C. These surface oxygen groups are products of decomposition of carboxylic or lactonic groups (Bansal *et al.*, 1988). CO was released with a peak at 690°C and shoulders between 300 and 950°C, which is the product of decomposition of phenolic or quinonic groups. The bulk sulfur content of AC-C2 decreased from 1.26 to 0.84 wt% after HNO_3 treatment (Table 2). This decrease resulted both from a mass dilution effect of adding 17 wt% oxygen to the AC and from the dissolution of sulfur functional groups by HNO_3. For AC-C2-HNO_3 (yield = 0.84 based on the starting mass of AC-C2), approximately 44 wt% of the precursor's total sulfur was dissolved in HNO_3.

HNO_3 treatment also altered the physical properties of ACs, but the changes were not so significant as those caused by low temperature elemental sulfur impregnation (Table 2). S_{BET} of AC-C2 decreased from 702 to 590 m^2/g most likely due to the addition of oxygen groups into AC's pores.

HNO_3 treatment significantly decreased the Hg adsorption capacities. The equilibrium Hg^0 adsorption capacities for AC-C2 decreased from 1758 to 334 μg/g after HNO_3 treatment (Table 2). Also the equilibrium $HgCl_2$ adsorption capacities of AC-C2 decreased from 657 to 64 μg/g. These results indicate that the addition of surface oxygen groups combined with the removal of almost half of the original sulfur content decreases Hg adsorption from the coal-combustion flue gas. S-XANES results for samples AC-C2 and AC-C2-HNO_3 suggested that sulfate, sulfone and sulfoxide were unlikely to be the active functional groups for Hg^0 adsorption because the quantities of these groups increased or remained constant after HNO_3 treatment, while Hg adsorption markedly decreased. Elemental sulfur is an oxidation product of pyrite (Duran *et al*., 1986), which is present in the AC precursors (pyrite sulfur = 0.4–1.1 wt%, Table 1). Thiophene is commonly present in coal-based ACs. Elemental sulfur, thiophene, and organic sulfide content of the AC decreased after HNO_3 treatment (Table 3). It appears, therefore, that elemental sulfur, thiophene, and organic sulfide are the active functional groups for Hg^0 adsorption because

Table 3. Sulfur functional groups of original and sulfur-impregnated activated carbons quantified by S-XANES examinations.

Sample Code	Elemental Sulfur	Pyrrhotite Sulfur	Sulfate	Organic Sulfide	Sulfoxide	Sulfone	Thiophene
				(wt%)			
AC107	0.01	0.00	0.09	0.19	0.11	0.01	1.23
AC109-2	0.03	0.00	0.11	0.08	0.04	0.04	0.51
AC-C2	0.13	0.00	0.12	0.00	0.03	0.00	0.98
AC109-2-120S-5	1.07	0.00	1.28	0.21	0.00	0.56	1.16
AC109-2-600S	3.21	1.06	1.43	0.00	0.35	0.52	5.43
AC-C2-HNO_3	0.09	0.00	0.11	0.00	0.02	0.13	0.51

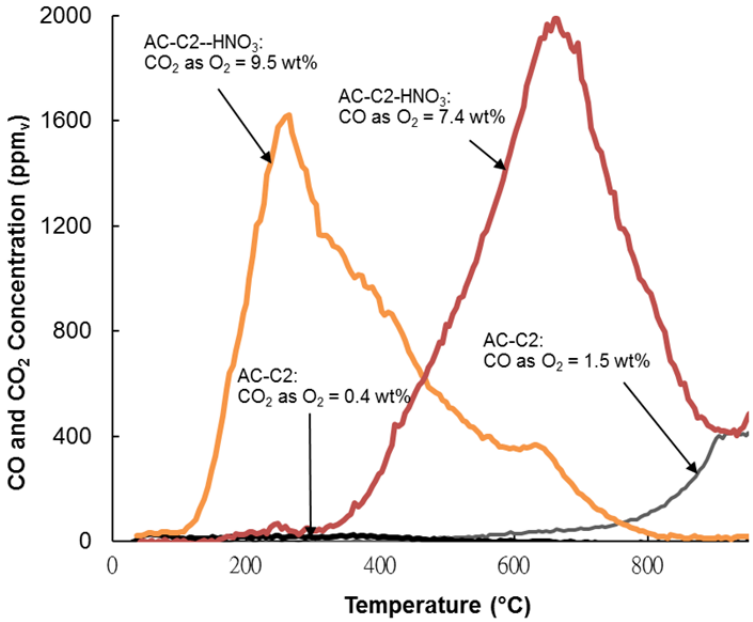

Fig. 3. TPD examinations of original and acid-treated carbons.

the decrease in the concentration of these groups is consistent with the decrease in Hg^0 adsorption after HNO_3 treatment. Note that an increase in AC's H_2O and SO_2 adsorption capacity after HNO_3 treatment may also contribute to the observed decrease in Hg^0 adsorption capacity (Daley *et al.*, 1997; Lizzio and DeBarr, 1997; Sullivan *et al.*, 2007). AC-C2 had an H_2O content of approximately 5 wt% while AC-C2-HNO_3 contained 14 wt% H_2O. Hg^0 is insoluble in H_2O (solubility = 6×10^{-5} g/L at 25°C) (Schuster, 1991). As a result, only 0.008 μg/g Hg^0 can partition into the HNO_3-treated AC if H_2O saturated the porous structure and Hg^0 only interacted with the water in the pores (i.e., no interaction with the solid phase); potentially increasing the resistance of Hg^0 diffusion into the pores of HNO_3-treated AC.

Effects of Thermal Treatment of the HNO_3-Treated Samples

Thermal treatment at 950°C desorbs oxygen and sulfur functional groups from ACs. Although the sulfur content of the TPD product (i.e., AC-C2-HNO_3-TPD) increased from 0.84 to 0.96 wt% (Table 2), the sulfur removal due to TPD treatment (sample yield = 0.51 based on the mass of AC-C2-HNO_3) was 42%. S_{BET}, V_t, and V_{micro} increased after thermal treatment due to desorption of oxygen functional groups (Table 2). The equilibrium Hg^0 adsorption capacities for AC-C2-HNO_3-TPD were 355 μg/g (Table 2), which is comparable to that of AC-C2-HNO_3. Compared to AC-C2 (1758 μg/g), however, the nascent carbon sites generated after releasing surface oxygen and sulfur groups were not active for Hg^0 adsorption in the simulated coal-combustion flue gas. Nevertheless, the increase in the amount of carbon nascent sites resulted in a greater $HgCl_2$ adsorption capacity than they were covered with the surface oxygen groups (Table 2).

Both the HNO_3- and thermal-treated ACs exhibited lower Hg adsorption capacities than untreated, high-organic-sulfur coal-derived ACs. These observations disagree with an earlier study, in which oxygen functional groups were shown to improve Hg^0 adsorption of ACs in a N_2 environment (Matsumura, 1974). In our study, Hg adsorption tests were performed in a simulated coal-combustion flue gas as described above. It is highly likely that some of the flue gas components (e.g., SO_2 and H_2O) preferentially react with surface oxygen groups and nascent carbon sites (Hoffman *et al.*, 1984; Daley *et al.*, 1997; Lizzio and DeBarr, 1997), resulting in a decrease in Hg adsorption capacity due to competitive adsorption/reaction at the AC's active sites. The interactions between Hg, flue gas components, and surface functional groups on the AC are complex. It remains to be determined what are the factors contributing to the adsorption equilibrium and kinetics of Hg onto ACs and whether a detailed understanding of these factors can be applied to produce highly efficient and cost-effective carbonaceous adsorbents to remove vapor-phase Hg in flue gases of coal-fired power plants.

CONCLUSIONS

This study describes how sulfur, HNO_3, and thermal treatments impact the Hg adsorption of coal-based activated carbon (AC) in a simulated coal-combustion flue gas. The results showed that equilibrium Hg^0 and $HgCl_2$ adsorption capacities for low-organic-sulfur ACs in general increased after high-temperature sulfur impregnation. Low-temperature sulfur impregnation (120°C and 200°C) using polysulfide or elemental sulfur decreased Hg^0 adsorption but increased $HgCl_2$ adsorption. These data suggest that AC's physical and chemical properties influence Hg^0 capture. $HgCl_2$ adsorption, however, is primarily controlled by the chemical characteristics (e.g., sulfur content) of ACs for the conditions reported here. HNO_3 and thermal treatments removed active sulfur functional groups and caused a decrease in Hg

capture. Elemental sulfur, thiophene, and organic sulfide appeared to be the active functional groups contributing to adsorption of Hg onto AC. HNO_3 and thermal treatment of ACs resulted in decreasing Hg^0 and $HgCl_2$ adsorption capacity, suggesting that Hg and flue gas components potentially compete for the same nascent carbon and surface oxygen groups adsorption sites.

ACKNOWLEDGMENTS

Funding support from EPRI and Taiwan NSC (97-2221-E-327-006-MY3) are greatly appreciated. The authors acknowledge the help of URS Corporation for Hg adsorption tests, Dr. Frank Huggins (University of Kentucky) for S-XANES examinations, and Mr. John Atkinson for his editorial contributions. The opinions expressed in this paper are not necessarily those of the sponsors.

REFERENCES

American Society for Testing and Materials (1988). Test Method for the Forms of Sulfur in Coal, ASTM D2492, *Annual Book of ASTM Standards*, 5.05, Philadelphia, PA.

Bansal, R.C., Donnet, J.B. and Stoeckli, F. (1988). *Active Carbon*, Marcel Dekker, New York.

Berkovitz, J. (1965). In *Elemental Sulfur Chemistry and Physics*, Meyer, B. (Ed.), Interscience, p. 125–159.

Bittrich, D.R., Rutter, A.P., Hall, B.D. and Schauer, J.J. (2011a). Photodecomposition of Methylmercury in Atmospheric Waters. *Aerosol Air Qual. Res.* 11: 290–298.

Bittrich, D.R., Chadwick, S.P., Babiarz, C.L., Manolopoulos, H., Rutter, A.P., Schauer, J.J., Armstrong, D.E., Collett, J. and Herckes, P. (2011b). Speciation of Mercury (II) and Methylmercury in Cloud and Fog Water. *Aerosol Air Qual. Res.* 11: 161–169.

Blayden, H.E. and Patrick, J.W. (1967). Solid Complexes of Carbon and Sulphur-l. Sulphurised Polymer Carbons. *Carbon* 5: 533–544.

Carey, T.R., Hargrove, O.W. Jr, Richardson, C.F., Chang, R. and Meserole, F.B. (1998). Factors Affecting Mercury Control in Utility Flue Gas using Activated Carbon. *J. Air Waste Manage. Assoc.* 48: 1166–1174.

Carpi, A. (1997). Mercury from Combustion Sources: A Review of the Chemical Species Emitted and Their Transport in the Atmosphere. *Water Air Soil Pollut.* 98: 241–254.

Daley, M.A., Mangun, C.L., DeBarr, J.A., Riha, S., Lizzio, A.A., Donnals, G.L. and Economy, J. (1997). Adsorption of SO_2 onto Oxidized and Heat-Treated Activated Carbon Fibers (ACFs). *Carbon* 35: 411–417.

Duran, J.E., Mahasay, S.R. and Stock, L.M. (1986). The Occurrence of Elemental Sulphur in Coals. *Fuel* 65: 1167–1168.

Fang, G.C., Tsai, J.H., Lin, Y.H. and Chang, C.Y. (2012). Dry Deposition of Atmospheric Particle-Bound Mercury in the Middle Taiwan. *Aerosol Air Qual. Res.* 12: 1298–1308.

Feng, W., Borguet, E. and Vidic, R.D. (2006a). Sulfurization of Carbon Surface for Vapor Phase Mercury Removal - II: Sulfur Forms and Mercury Uptake. *Carbon* 44: 2998–3004.

Feng, W., Kwon, S., Feng, X., Borguet, E. and Vidic, R.D. (2006b). Sulfur Impregnation on Activated Carbon Fibers through H_2S Oxidation for Vapor Phase Mercury Removal. *J. Environ. Eng.* 132: 292–300.

Ghorishi, S.B. and Sedman, C.B. (1998). Low Concentration Mercury Sorption Mechanisms and Control by Calcium-Based Sorbents. *J. Air Waste Manage. Assoc.* 48: 1191–1198.

Ho, T.C., Shetty, S., Chu, H.W., Lin, C.J. and Hopper, J.R. (2008). Simulation of Mercury Emission Control by Activated Carbon under Confined-Bed Operations. *Powder Technol.*180: 332–338.

Hoffman, W.P., Vastola, F.J. and Walker, P.L. Jr (1984). Chemisorption of Alkanes and Alkenes on Active Sites. *Carbon* 22: 585–594.

Hsi, H.C., Chen, S., Rostam-Abadi, M., Rood, M.J., Richardson, C.F., Carey, T.R. and Chang, R. (1998). Preparation and Evaluation of Coal-Derived Activated Carbons for Removal of Mercury Vapor from Simulated Coal Combustion Flue Gases. *Energy Fuels* 12: 1061–1070.

Hsi, H.C., Rood, M.J., Rostam-Abadi, M., Chen, S. and Chang, R. (2001). Effects of Sulfur Impregnation Temperature on the Properties and Mercury Adsorption Capacities of Activated Carbon Fibers (ACFs). *Environ. Sci. Technol.* 35: 2785–2791.

Hsi, H.C., Rood, M.J., Rostam-Abadi, M., Chen, S. and Chang, R. (2002). Mercury Adsorption Properties of Sulfur-Impregnated Adsorbents. *J. Environ. Eng.* 128: 1080–1089.

Hsi, H.C., Tsai, C.Y., Kuo, T.H. and Chiang, C.S. (2011). Development of Low-Concentration Mercury Adsorbents from Biohydrogen-Generation Agricultural Residues Using Sulfur Impregnation. *Bioresour. Technol.* 102: 7470–7477.

Huggins, F.E., Vaidya, S.V., Shah, N. and Huffman, G.P. (1993). Investigation of Sulfur Forms Extracted from Coal by Perchloroethylene. *Fuel Process. Technol.* 35: 233–257.

Karatza, D., Lancia, A. and Musmarra, D. (1998). Fly Ash Capture of Mercuric Chloride Vapors from Exhaust Combustion Gas. *Environ. Sci. Technol.* 32: 3999–4004.

Korpiel, J.A. and Vidic, R.D. (1997). Effect of Sulfur Impregnation Method on Activated Carbon Uptake of Gas-Phase Mercury. *Environ. Sci. Technol.* 31: 2319–2325.

Krishnan, S.V., Gullett, B.K. and Jozewicz, W. (1994). Sorption of Elemental Mercury by Activated Carbons. *Environ. Sci. Technol.* 28: 1506–1512.

Lancia, A., Musmarra, D., Pepe, F. and Volpicelli, G. (1993). Adsorption of Mercuric Chloride Vapours from Incinerator Flue Gases on Calcium Hydroxide Particles. *Combust. Sci. Technol.* 93: 277–289.

Li, Y.H., Lee, C.W. and Gullett, B.K. (2003). Importance of Activated Carbon's Oxygen Surface Functional Groups on Elemental Mercury Adsorption. *Fuel* 82: 451–457.

Lippens, B.C. and de Boer, J.H. (1965). Studies on Pore Systems in Catalysts: V. The t Method. *J. Catal.* 4: 319–323.

Liu, W., Vidic, R.D. and Brown, T.D. (1998). Optimization of Sulfur Impregnation Protocol for Fixed-Bed Application of Activated Carbon-Based Sorbents for Gas-Phase Mercury Removal. *Environ. Sci. Technol.* 32: 531–538.

Liu, W., Vidic, R.D. and Brown, T.D. (2000). Optimization of High Temperature Sulfur Impregnation on Activated Carbon for Permanent Sequestration of Elemental Mercury Vapors. *Environ. Sci. Technol.* 34: 483–488.

Lizzio, A.A. and DeBarr, J.A. (1997). Mechanism of SO_2 Removal by Carbon. *Energy Fuels* 11: 284–291.

Maes, I.I., Mitchell, S.C., Yperman, J., Franco, D.V., Marinov, S.P., Mullens, J. and Van Poucke, L.C. (1996). Sulfur Functionalities and Physical Characteristics of the Maritza Iztok Basin Lignite. *Fuel* 75: 1286–1293.

Matsumura, Y. (1974). Adsorption of Mercury Vapor on the Surface of Activated Carbons Modified by Oxidation or Iodization. *Atmos. Environ.* 8: 1321–1327.

Pacyna, E.G., Pacyna, J.M., Sundseth, K., Munthe, J., Kindbom, K., Wilson, S., Steenhuisene, F. and Maxson, P. (2010). Global Emission of Mercury to the Atmosphere from Anthropogenic Sources in 2005 and Projections to 2020. *Atmos. Environ.* 44: 2487–2499.

Peise, O., Ji, L., Thiel, S.W. and Pinto, N.G. (2008). New Adsorbents for Direct Warm-Gas Capture of Mercury. *Main Group Chem.* 7: 181–189.

Puri, B.R. and Hazra, R.S. (1971). Carbon Sulphur Surface Complexes on Charcoal. *Carbon* 8: 123–134.

Schuster, E. (1991). The Behavior of Mercury in the Soil with Special Emphasis on Complexation and Adsorption Processes - A Review of the Literature. *Water Air Soil Pollut.* 56: 667–680.

Staudt, J.E. and Jozewicz, W. (2003). *Performance and Cost of Mercury and Multipollutant Emission Control Technology Applications on Electric Utility Boilers*, EPA-600/R-03-110, Research Triangle Park, NC.

Sullivan, P.D., Stone, B.R., Hashisho, Z. and Rood, M.J. (2007). Water Adsorption with Hysteresis Effect onto Microporous Activated Carbon Fabrics. *Adsorption* 13: 173–189.

Sun, J., Chen, S., Rood, M.J. and Rostam-Abadi, M. (1998). Correlating N_2 and CH_4 Adsorption on Microporous Carbon Using a New Analytical Model. *Energy Fuels* 12: 1071–1078.

Tuller, W.N. (1954). *The Sulphur Data Book*, McGraw-Hill, New York.

U.S. Environmental Protection Agency website. Available at http://www.epa.gov/air/mercuryrule/ (accessed December 2011).

Vitolo, S. and Seggiani, M. (2002). Mercury Removal from Geothermal Exhaust Gas by Sulfur-Impregnated and Virgin Activated Carbons. *Geothermics* 31: 431–442.

Wu, Y.L., Rahmaningrum, D.G., Lai, Y.C., Tu, L.K., Lee, S.J., Wang, L.C. and Chang-Chien, G.P. (2012). Mercury Emissions from a Coal-Fired Power Plant and Their Impact on the Nearby Environment. *Aerosol Air Qual. Res.* 12: 643–650.

Received for review, July 10, 2012
Accepted, November 19, 2012